Final Report (9/15/2011 – 9/14/2015)

Collaborative Project: Development of hybrid 3-D hydrological modeling for the NCAR Community Earth System Model (CESM)

DOE Program: SciDAC Program, Climate & Environmental Sciences Division

DOE Program Manager: Dorothy M. Koch

Overall Project PI: Xubin Zeng (University of Arizona)

Total Budget: $761,725

University of Arizona

PI: Xubin Zeng

University of Arizona, Department of Atmospheric Sciences, Tucson, AZ 85721; Email: xubin@atmo.arizona.edu; Tel: 520-621-4782

Co-PI: Peter Troch, Jon Pelletier, and Guo-Yue Niu

DOE Grant Number: DE-SC0006773

National Center for Atmospheric Research (NCAR)

PI: David Gochis

NCAR Research Applications Laboratory (RAL), P.O. Box 3000, Boulder, CO 80307-3000; Email: gochis@ucar.edu; Tel: 303-497-2809]

DOE Grant Number: DE-SC0006779

Submitted to DOE on 11/15/2015

1. Introduction

This is the Final Report of our four-year (3-year plus one-year no cost extension) collaborative project between the University of Arizona (UA) and the National Center for Atmospheric Research (NCAR). The overall objective of our project is to develop and evaluate the first hybrid 3-D hydrological model with a horizontal grid spacing of 1 km for the NCAR Community Earth System Model (CESM).

We have made substantial progress in model development and evaluation, computational efficiencies and software engineering, and data development and evaluation, as discussed in **Sections 2-4**.

Section 5 presents our success in data dissemination, while **Section 6** discusses the scientific impacts of our work. **Section 7** discusses education and mentoring success of our project, while **Section 8** lists our relevant DOE services. All peer-reviewed papers that acknowledged this project are listed in **Section 9**.

Highlights of our achievements include:

- We have finished 20 papers (most published already) on model development and evaluation, computational efficiencies and software engineering, and data development and evaluation
- The global datasets developed under this project have been permanently archived and publicly available
- Some of our research results have already been implemented in WRF and CLM
- Patrick Broxton and Michael Brunke have received their Ph.D.
- PI Zeng has served on DOE proposal review panels and DOE lab scientific focus area (SFA) review panels

2. Model development

2.1 Hybrid 3-D model development

Through much effort, we have developed the prototype hybrid 3-D (h3D) hydrological model, as indicated by three papers/manuscripts.

Hazenberg et al. (2015a) developed a pseudo 3-D model to simulate the hydrological response of hillslopes by coupling a vertical column model with the lateral hillslope storage Boussinesq model. Hillslope-scale rainfall-runoff processes leading to a fast catchment response are not explicitly included in land surface models (LSMs) for use in earth system models (ESMs) due to computational constraints. This study presents the hillslope component of the hybrid-3D hydrological model that couples a 1D vertical soil column model with a lateral pseudo-2D saturated zone and overland flow model for use in ESMs (h3D-hillslope). By representing vertical and lateral responses separately at different spatial resolutions, the model is computationally efficient.

The h3D-hillslope model was first tested for three different hillslope planforms (uniform, convergent and divergent). We then compared h3D-hillslope (with single and multiple soil columns) with a complex physically-based 3D model and a simple 1D soil moisture model coupled with an unconfined aquifer (1c-CLM, as typically used in LSMs).

Figure 1 shows that simulations obtained by the simple 1D model vary considerably from the complex 3D model CATHY and are not able to represent hillslope-scale variations in the lateral flow response. In contrast, the single soil column h3D-hillslope model shows a much better performance and saves computational time by 2-3 orders of magnitude compared with the complex 3D model. When multiple vertical soil columns are implemented (20c-h3D-hillslope), the resulting hydrological responses (soil moisture, water table depth, and baseflow along the hillslope) from h3D-hillslope are nearly identical to those predicted by the complex 3D model, but still saves computational time. As such, the computational efficiency of the h3D-hillslope model provides a valuable and promising approach to incorporating hillslope-scale hydrological processes into continental and global-scale ESMs.

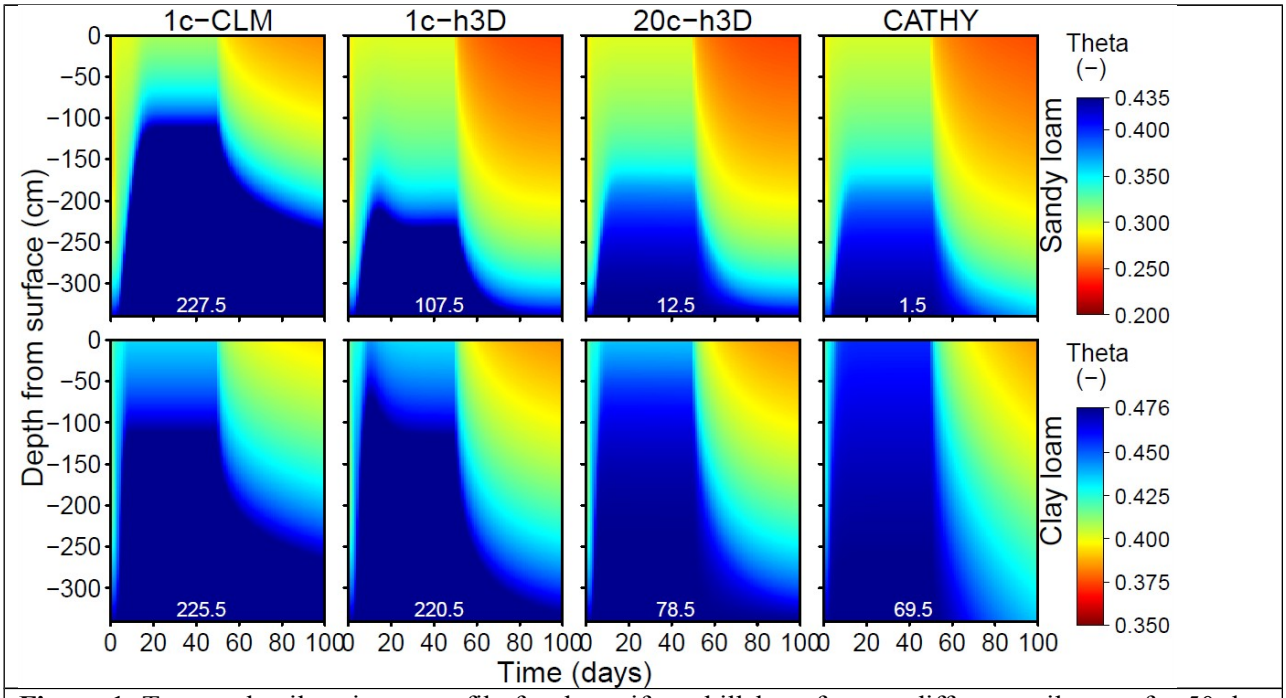

Figure 1: Temporal soil moisture profile for the uniform hillslope for two different soil types for 50 day recharge and 50 day drainage experiment. The white number at the bottom of each panel describes the depth of the saturated zone (cm) at the end of the recharge period. Note that for the 20c-h3D and CATHY model the average value of the lateral variations in the vertical soil column are presented (from Hazenberg et al. 2015a).

Hazenberg et al. (2015b) further assessed the performance of the hybrid-3D hillslope hydrological model (h3D-hillslope) using a number of recharge-drainage experiments within the Landscape Evolution Observatory (LEO) with accurate and high-resolution (both temporally and spatially) observations of the inputs, outputs and storage dynamics of several hillslopes. Such detailed measurements are generally not available for real-world hillslopes.

Figure 2 shows that the h3D-hillslope model captures the observed storage, baseflow, and overland flow dynamics of both the larger LEO and smaller miniLEO hillslope very well. Furthermore, improved overland flow simulations are obtained as compared to the full 3D model CATHY. Sensitivity tests are also performed to understand the model's difficulty in representing the height of the saturated zone close to the seepage face of the miniLEO hillslope. Results reveal that a temporally constant parameters set is well able to simulate the response of the miniLEO for each individual event. However, in case one focuses on the saturated zone dynamics at ~15 cm from the seepage face, a step-wise evolution of the optimal model parameter for the saturated lateral conductivity parameter of the gravel layer occurs. This

evolution might be related to the migration of soil particles within the hillslope. However, it is currently unclear whether this takes place (in the seepage face or within the parts of the loamy sand soil).

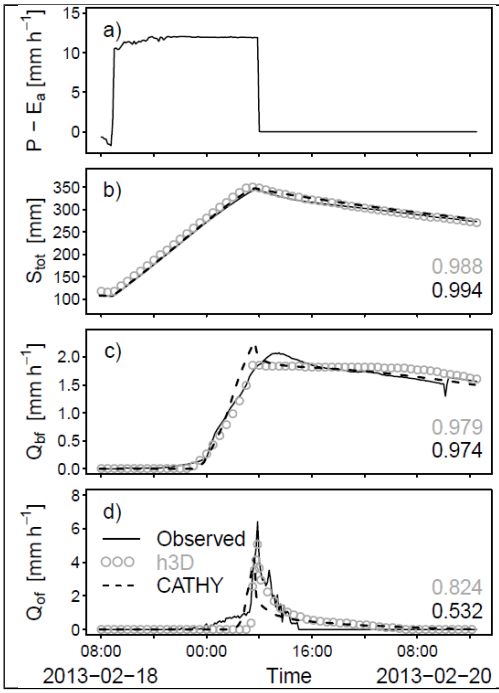

Figure 2: Timeseries of the observed (black line) and simulated hydrological response of h3D-hillslope (open circles) and 3D-Richards model CATHY (dashed line). Panel a) shows the atmospheric boundary flux P-Ea (mm h-1, panel b) the total vertical storage Stot [mm], panel c baseflow response Qbf [mm h-1] and panel d) the overland flow response Qof [mm h-1] as observed during a recharge-drainage experiment for the LEO hillslope. The performance of both models is represented by the Nash-Sutcliffe coefficient on the bottom right of panels b-d (from Hazenberg et al. 2015b).

Built on the work of Hazenberg et al. (2015a,b), **Hazenberg et al. (2015c)** presented the development of the h3D hydrogical model (**Figure 3**). This model was developed to represent the lateral hydrological response (e.g. groundwater, overland flow and river network) at hyperresolution (~1 km pixel resolution) while interacting with the vertical component as currently available in many LSMs. Since we are aware that even at these resolutions it is important to account for small scale hydrological processes, each pixel is further differentiated in a hillslope and flatland (e.g. riparian zone or low land) component.

In this work the scaling performance of the h3D hydrogical model is tested by implementing the model at different pixel resolutions (1, 2, 5 and 10 km) and comparing results with the full 3D Richard solution model CATHY. Furthermore, we have begun coupling parts of the h3D model with the NOAH-MP land surface model within the WRF-Hydro coupling environment. The performance of the coupled NOAH-MP - h3D model will be tested for the Delaware river basin.

2.2 An integrated modeling framework of catchment-scale ecohydrological processes

To evaluate the accuracy and efficiency of the hybrid-3D hydrological model developed in this project, we also need to develop the modeling capability based on the 3-D Richards equation with a horizontal grid spacing of meters to tens of meters. And we have made much progress in this area, as indicated by three papers.

Niu et al. (2013a,b) have developed a fully integrated catchment-scale ecohydrological model consisting of a 3-dimensional (3-D) Richards equation-based hydrological model and a land surface model (LSM). The model has been tested over an energy-limited catchment (8.4 km^2) of the Sleepers River watershed in Vermont (Niu et al., 2013a) and a water-limited catchment (7.92 ha) in southeastern Arizona (Niu et al., 2013b).

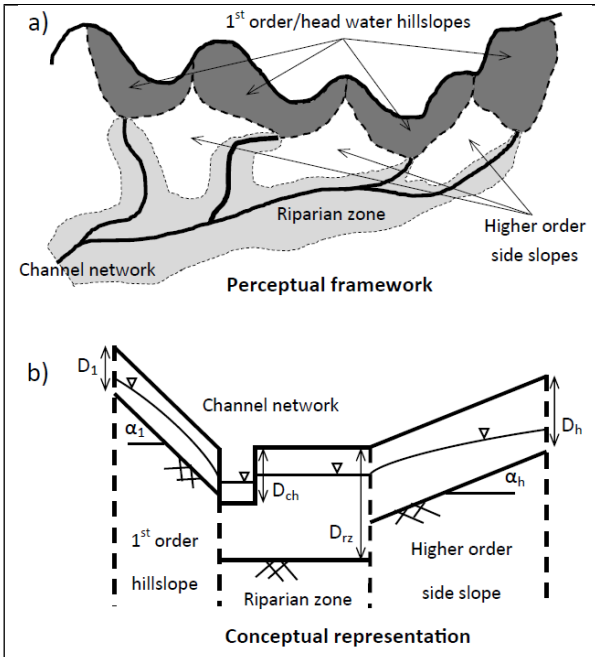

Figure 3: In panel (a) a perceptual representation of the small-scale hydrological variability within a given high-resolution grid cell (~0.1-1km) is given for a hilly/mountainous environment. The conceptual representation as implemented in the hybrid-3D model is given in panel (b), where only the dominant hydrological components are taken into account, while making use of the available hydrological and geomorphological information (from Hazenberg et al. 2015c).

The model is demonstrated to reproduce terrestrial surface energy, water, and carbon state and processes, including snow mass, soil moisture, river discharge, surface water heights and flooded area, surface energy, water, and carbon flux exchanges with the atmosphere (**Figure 4**). Through modeling in the water-limited catchment, we found that the wetter soils in lowland areas along stream rills and channels are results of re-infiltration of lateral overland flow. This water subsidy provides plants with favorable conditions to produce more leaves, CO_2, and evapotranspiration fluxes in lowland areas. Re-infiltration of overland flow over complex terrain may play a role in buffering the climatic impacts in a warming climate with less and more intense rainfall in the southwest US.

The 3D physically based hydrological model CATHY as used in Hazenberg et al. (2015b) was also used in **Niu et al. (2014)** to study the incipient subsurface heterogeneity and its effect on overland flow generation in LEO. Our null hypothesis is that the soil is hydraulically homogeneous, while the alternative hypothesis is that LEO developed downstream heterogeneity from transport of fine sediments driven by saturated subsurface flow.

The best model runs under the heterogeneous soil hypothesis produce smaller errors than those under the null hypothesis, and that the heterogeneous runs yield a higher probability of best model performance than the homogeneous runs. These results support the alternative hypothesis of localized incipient heterogeneity of the LEO soil, which facilitated generation of overland flow. This modeling study of the first LEO experiment suggests an important role of coupled water and sediment transport processes in the evolution of subsurface heterogeneity and on overland flow generation, highlighting the need of a coupled modeling system that integrates across disciplinary processes.

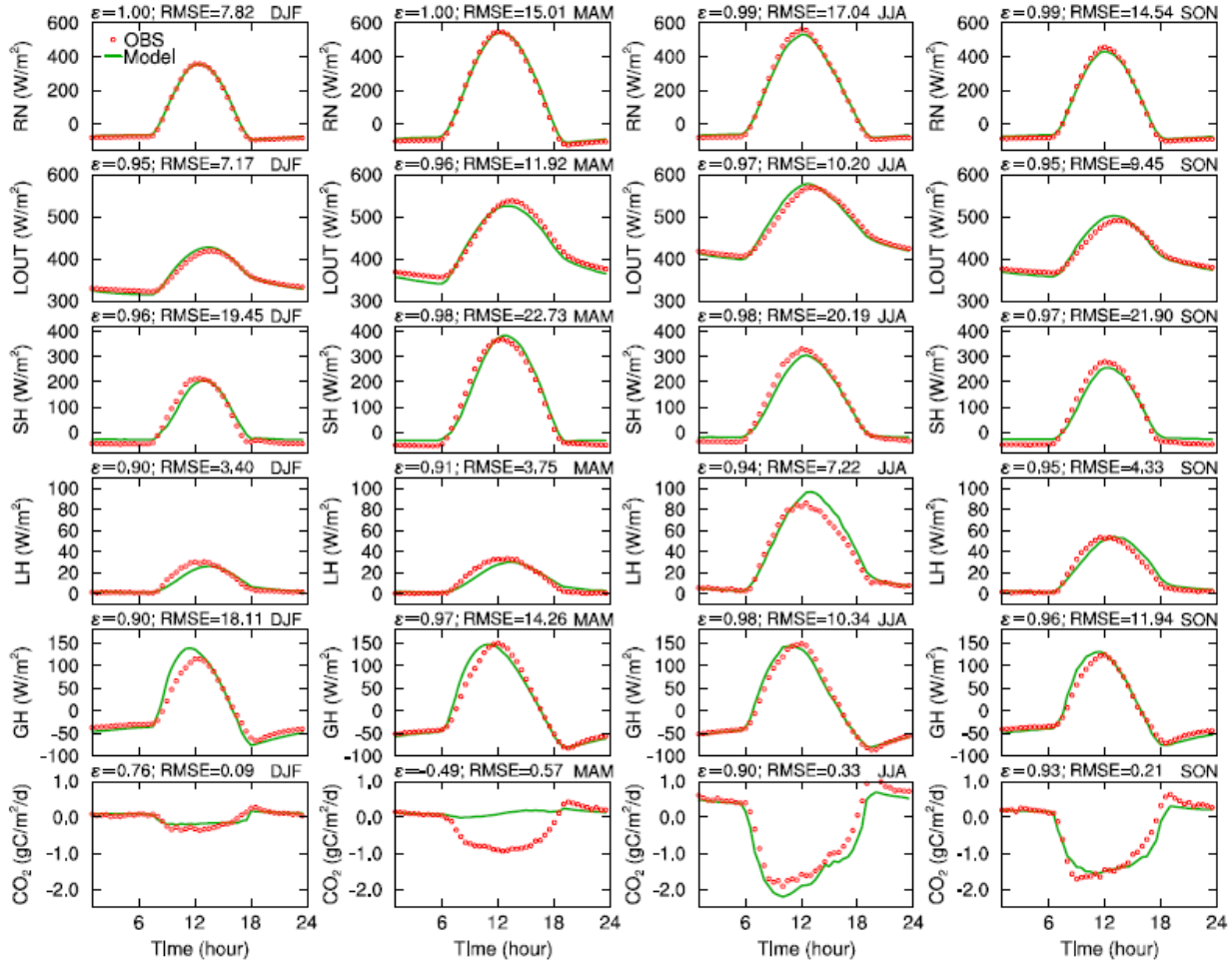

Figure 4. Comparison of observed (OBS) and modelled (by CTRL) diurnal variations in fluxes of net radiation (RN), outgoing longwave radiation (LOUT), sensible heat (SH), latent heat (LH), ground heat (GH), and CO2 averaged over all winters (DJF; December, January, and February), springs (MAM; March, April, and May), summers (JJA; June, July, and August), and falls (SON; September, October, and November) of the entire modeling period (from 6 May 2004 to the end of 2009) at the Kendall subwatershed of Walnut Gulch, Arizona (from Niu et al. 2013b).

2.3 A simple model for monthly river flow forecasting

Besides the hybrid 3-D hydrological model, we have also developed a simple model for monthly river flow forecasting using the river flow and river basin averaged precipitation in the prior month (**Zeng et al. 2012**). Model coefficients are calibrated for each month using historical data. This model is based on water balance, easy to use and reproduce, and robust to calibrate with a short period of data. For five major rivers in the world, its results agree with observations very well. Its prediction uncertainty can be quantified using the model's error statistics or using a dynamic approach, but not by the dispersion of 10,000 ensemble members with different sets of coefficients in the model. Its results are much better than those from a physically based land model (CLM) even after the mean bias correction. This model and a standard neural network available from MATLAB give similar results, but the latter is more sensitive to the length of calibration period. For the monthly prediction of river flow with a strong seasonal cycle, a modified Nash-Sutcliffe coefficient of efficiency is introduced and is found to be more reliable in model evaluations than the original coefficient of efficiency or the correlation coefficient.

2.4 A flash flood model for rain-on-snow flooding

Broxton et al. (2014a) developed an all-season flash-flood forecasting system to improve flash flood prediction in catchments where snowmelt and rain-on-snow precipitation events are important in some floods. The system used an overland flow and channel routing model coupled with a hillslope subsurface flow and snowmelt model and was run at high spatial and temporal resolutions. The model was set up to run in real-time using NWS forecasts to predict streamflow up to 24 hours into the future in the Upper Delaware Basin, in southeastern New York for experimental use by scientists at the National Weather Service Binghamton Weather Forecast Office.

3. Computational tasks

3.1 Efficient numerical schemes

We have made much progress in the efficient numerical scheme of the newly proposed hydrological framework (**Hazenberg et al. 2015a**) and in the vertical direction (**Brunke et al. 2015**). In particular, **Brunke et al. (2015)** have extended the traditional global fixed soil column depth in CLM to incorporate spatially variable soil depth information. A globally available depth to bedrock dataset, which has been developed as part of our DOE-SciDAC project, is used to determine how many layers are needed for each grid cell in this version of CLM and compared to the traditional setup.

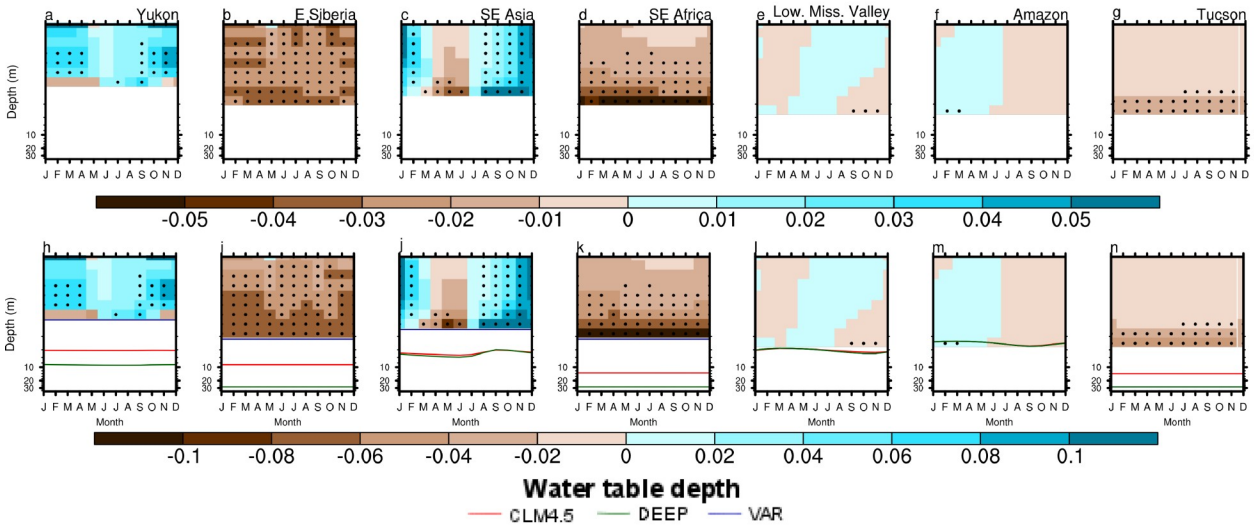

Figure 5: The mean annual cycles of the difference in (a-g) volumetric soil moisture content, θ, and (h-n) fraction of saturation, θ / θ_{sat}, between versions of CLM4.5 with and without variable soil thickness for the grid cells containing the locations indicated in the top row. Dots are given in each grid cell in which the difference is statistically significant at the 90% level according to a Student's t-test. The horizontal lines in the bottom row of panels represent the mean annual cycle in water table depth (WTD) in out-of-the box CLM4.5 (red), a version with a constant soil thickness at ~28 m (DEEP, green), and another with variable soil thickness (VAR, blue) (from Brunke et al. 2015).

Results show large differences between both approaches, especially for regions with shallow bedrock and even in some regions where the bedrock is deep. For instance, **Figure 5** shows that soil moisture in CLM with variable soil thickness is most sensitive at locations where the number of soil layers is reduced from the standard constant 10 in the out-of-the-box version (the leftmost four columns). Soil moisture is

mostly unchanged in the profiles from the two wet locations where the soil column is deepened (the Lower Mississippi Valley and the Amazon). Such soil moisture changes result in large changes to baseflow with the annual maximum generally occurring earlier and in smaller changes to surface runoff primarily due to a change in the annual cycle amplitude. An added benefit is to the soil temperature profiles due largely to the soil moisture profile changes and also to changes in the vertical distribution to heat capacity and conductivity. These changes result in increases in the amplitude of the mean annual cycle of soil temperature in regions where the bedrock is shallow and reductions in the amplitude in deeper layers where the bedrock is deep.

3.2 Software engineering

We have also made much progress in software engineering to enable 'process-based' hydrologic modeling within CESM. First, we have expanded the functionality of the WRF-Hydro coupling architecture to be compatible with a variety of Earth System modeling platforms. Second, we have built the underlying geospatial database and model pre-processing tools to conduct continental scale model experiments. Third, we have implemented and tested the WRF-Hydro coupling architecture in the Delaware River test basin as a demonstration of process interoperability. Finally, we have built the model forcing dataset and associated pre-processing tools for conducting our project's test simulations over the Delaware River and, eventually, continental scale model experiments. These efforts have been implemented in **Hazenberg et al. (2015c)**.

4. Data development and model evaluations

4.1 Soil and topographic attributes datasets

Pelletier et al. (2015) developed a high-resolution gridded global dataset of the average thickness of soil, intact regolith, and sedimentary deposits within each 30 arcsecond (~1 km) pixel using high-resolution (up to 3 arcsecond (~90 m)) data for topography, climate, and geology as input. Our dataset partitions the global land surface into upland hillslope, upland valley bottom, and lowland landscape components based on geologic and topographic criteria.

Then, it uses models optimized for each landform type to estimate the thicknesses soil and alluvium globally (**Figure 6**). The thickness of soil/alluvium in lowlands is predicted based on a relationship with topographic roughness, in upland valleys, it is predicted from the curvature of the valley bottom and the gradient of the hillslopes flanking the valley; and on upland hillslopes, it is predicted using geomorphic/pedogenic models that are based on topography and climate. On hillslopes, the dataset is calibrated and validated using independent datasets of measured soil thicknesses from the U.S. and Europe and on lowlands using depth to bedrock observations from groundwater wells in the U.S. We anticipate that the dataset will prove useful as an input to regional and global hydrological and ecosystems models.

In addition to our soil depth dataset, we have developed a method for extracting channel networks from high resolution topographic data **(Pelletier, 2013).** The method only requires two parameters, and produces accurate results in multiple settings with a consistent parameter set, suggesting its applicability for large areas. Furthermore, we have developed preliminary data for other soil and topographic attributes.
The bedrock depth data were also used in the CLM model sensitivity test described above **(Brunke et al., 2015).**

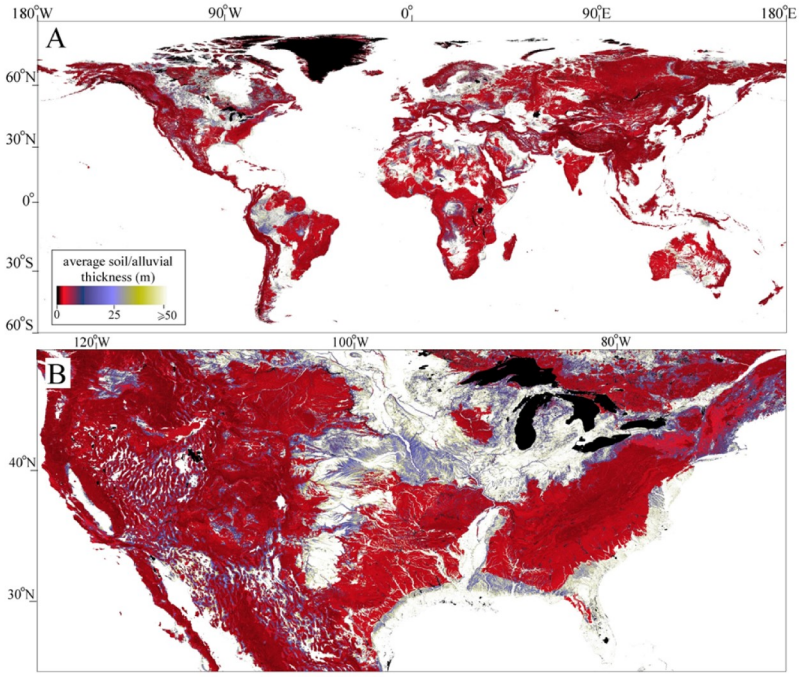

Figure 6: Maps of the average of soil and alluvial thicknesses within each pixel. (a) Global map, (b) subset of (a) for the conterminous U.S. (from Pelletier et al. 2015).

4.2 Global vegetation dataset

Consistent with our 1 km soil dataset, **Broxton et al. (2014b)** developed a global 0.5 km land cover type dataset based on 10 years of MODIS satellite data. The original MODIS data upon which our dataset is based had a large amount of spurious interannual variability. For example, 40% of land pixels changed land cover type one or more times during 2001–10 **(Figure 7a).** This affects the global distribution of vegetation if any one year or many years of data are used, for example, to parameterize land processes in regional and global models. We found that the MODIS data could be improved by combining multiple years of data using per-pixel confidence scores.

This dataset **(Figure 7b)** agrees with in situ validation data better than the original MODIS data for individual years. It also validates better than the Global Land Cover Characteristics (GLCC) database, which is based on 1 year of AVHRR data and represents a widely used first-generation global product. This dataset has been implemented in version 3.6 of the Weather Research and Forecasting (WRF) model, has been permanently archived at the USGS, and will be implemented in CLM5.0.

Broxton et al. (2014c) developed a global 1 km Maximum Green Vegetation Fraction (MGVF) product based on a climatology of MODIS normalized difference vegetation index (NDVI) and the Land Cover (LC) type data described above. There are substantial differences between our climatology and MGVF data from the MODIS Continuous Fields collection 4v3 data, which is currently used in the Community Land Model (CLM). While it is difficult to judge which product is more realistic due to lack of ground truth, our new MGVF product has the advantage of being more consistent than with the MODIS Leaf Area Index (LAI) product than is the Continuous Fields data. This consistency is important because both MGVF and LAI are measures of vegetation abundance and within given land cover types, it does not make sense to have LAI decrease as MGVF increases and vice versa. This dataset has been permanently archived at the USGS.

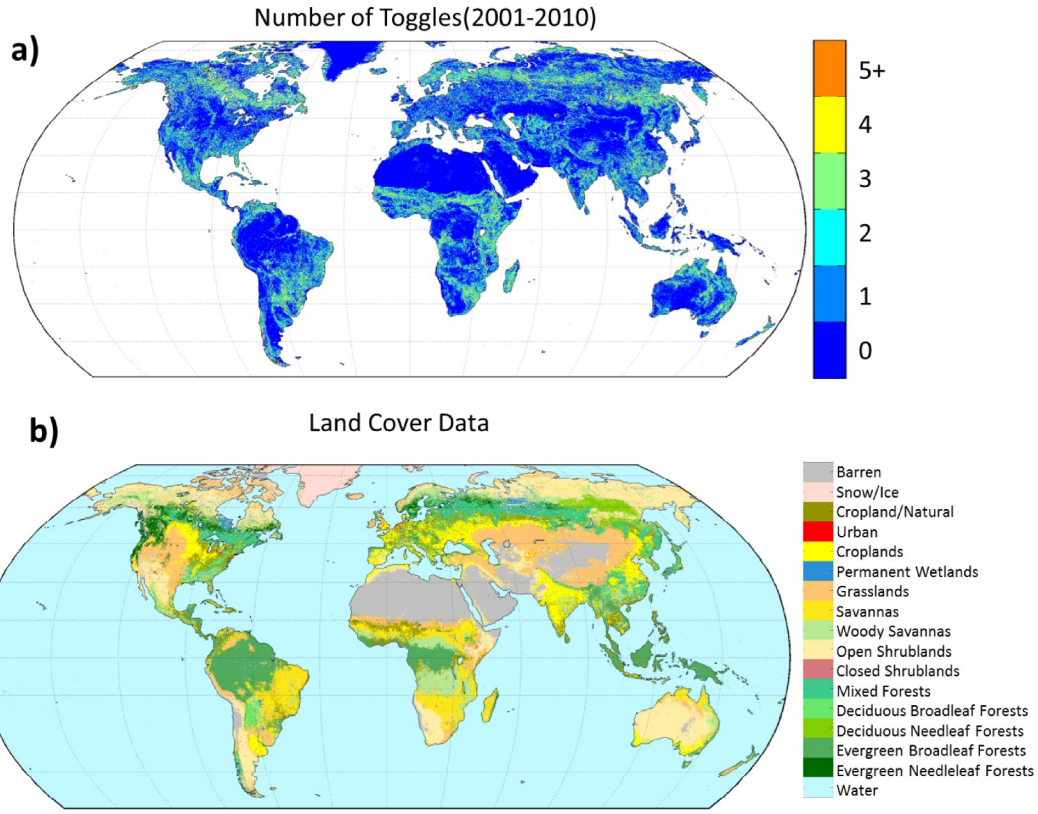

Figure 7: a) the number of toggles (or switches) between vegetation types from 2001 to 2010 in the original MODIS data. b) shows the land cover dataset after the yearly MODIS data has been merged (from Broxton et al. 2014b).

4.3 0.5˚ hourly land surface air temperature data

Global 0.5˚ monthly averaged data of daily maximum (Tx), minimum (Tn), and mean [Tm = (Tx + Tn)/2] land surface air temperature (Ta) are one of the most important observational datasets in climate study. For a variety of applications, the Ta diurnal cycle and day-to-day variation are also needed. We have come up with a new idea to develop a global 0.5˚ hourly Ta data from 1948-2009 based on the CRU TS3.10 in situ data as well as MERRA, ERA-40, ERA-Interim, and NCEP reanalysis data. First, we have published an AGU Eos Forum article (**Zeng and Wang 2012**) to argue, from scientific, technological, and historical perspectives, that it is time to compute the true monthly mean using hourly data for the national and international climate data record. Second, we have published one paper (**Wang and Zeng 2013**) to document our datasets.

Using this dataset, **Wang and Zeng (2014)** introduced the range of monthly averaged hourly temperature diurnal cycle (RMDT) as a new and complementary metric compared with the existing metric of monthly averaged diurnal temperature range (MDTR). RMDT in January is found to be much smaller than that in July over high northern latitudes, as it is much more affected by the diurnal radiative forcing than by the horizontal advection of temperature. In contrast, MDTR in January is comparable to that in July over high northern latitudes, but it is much larger than January RMDT, as it primarily reflects the movement of lower-frequency synoptic weather systems. The RMDT trends in November, December, and January north of 40˚N are near zero, while the trends of MDTR are negative.

Also using this dataset, **Wang and Zeng (2015)** quantified the spatiotemporal characteristics of four newly developed hourly temperature products by merging reanalysis with in situ data Climatic Research Unit (CRU) (Wang and Zeng 2013). Overall, LSATs from different hourly products are consistent with each other, and their differences are generally smaller in magnitude than biases between hourly products and monthly averaged daily maximum and minimum temperature data from CRU. While the true monthly mean (using hourly values) and the monthly mean (of daily maximum and minimum temperatures) and their seasonality [as represented by the (July–January) differences] differ, their trends agree with each other very well.

The polar amplification ratio of average temperature trend north of 65°N to that over global land (excluding Greenland and Antarctica) is also similar among different products, with the annual ratio of around 1.7. The ratio in summer (June–August) is always smaller than the annual value for different periods among all products. Based on the probability distribution functions from the monthly anomalies of different variables, the coldest tenth percentile of temperature in each decade overall increases with time, while the warmest tenth percentile does not vary much from 1950–1979, followed by a rapid increase from 1980–2009. These results and additional sensitivity tests suggest that the four hourly LSAT products can be widely used for climate analysis, model evaluation, and offline land surface modelling from 1948–2009.

4.4 Soil respiration in land models

Soil microbial respiration pulses in response to episodic rainfall pulses (the “Birch effect”) are poorly understood. **Zhang et al. (2014)** developed and assessed five evolving microbial enzyme models against field measurements from a semiarid savannah characterized by pulsed precipitation to understand the mechanisms to generate the Birch pulses. The five models evolve from an existing four-carbon (C) pool model to models with additional C pools and explicit representations of soil moisture controls on C degradation and microbial uptake rates.

Assessing the models using techniques of model selection and model averaging suggests that models with additional C pools for accumulation of degraded C in the dry zone of the soil pore space result in a higher probability of reproducing the observed Birch pulses. Degraded C accumulated in dry soil pores during dry periods becomes immediately accessible to microbes in response to rainstorms, providing a major mechanism to generate respiration pulses. Explicitly representing the transition of degraded C and enzymes between dry and wet soil pores in response to soil moisture changes and soil moisture controls on C degradation and microbial uptake rates improve the models' efficiency and robustness in simulating the Birch effect. Assuming that enzymes in the dry soil pores facilitate degradation of complex C during dry periods (though at a lower rate) results in a greater accumulation of degraded C and thus further improves the models' performance. However, the actual mechanism inducing the greater accumulation of labile C needs further experimental studies.

4.5 IPCC model surface air temperature evaluation

The climate models that participated in the IPCC fourth assessment report (AR4) have been intensively studied, but temporal or spatial scale limits for their prediction skill have rarely been systematically analyzed. With increasing interests and demands for regional and decadal scale predictions, we attempt to quantify the spatial and temporal scale dependence of the long-term global climate simulations by comparing the trends of annual mean surface air temperature from two observational data and 20th century simulations for AR4 over several temporal and spatial scales. A major conclusion is that robust climate signals at 30° or larger spatial scales and 40 years or longer temporal scales can be reproduced by the multi-model ensemble mean of AR4 - generation models. The spatial and temporal distributions of

some persistently large errors are also found in the northern high latitudes (**Sakaguchi et al. 2012a**). The conclusions remain the same using AR5 (or CMIP5)-generation models. In particular the model improvement from AR4-generation to AR5-generation was addressed. The second paper has also been published (**Sakaguchi et al. 2012b**).

4.6 Land model review

Niu and Zeng (2012) reviewed the land component of earth system models as a book chapter of Encyclopedia of Sustainability Science and Technology.

5. Data dissemination

We have made excellent progress in releasing our data to the community:

- Our global 0.5° hourly land surface air temperature data (Wang and Zeng 2013) (with a total volume of 1.5 Tb of data) are permanently archived and available at http://rda.ucar.edu/datasets/ds193.0/.

- The global 0.5 km land cover data (Broxton et al., 2014a) are permanently archived and available at http://landcover.usgs.gov/global_climatology.php

- The global 1 km green vegetation cover data (Broxton et al., 2014b) are permanently archived available at http://landcover.usgs.gov/green_veg.php

- The global 1 km bedrock depth data (Pelletier et al., 2015) will be permanently archived and available at ORNL once the manuscript is accepted for publication.

6. Scientific impact of our work

Besides the scientific impacts of our work through peer-reviewed publications in Section 9, some of our results have been implemented in community models:

- We have worked with the community Weather Research and Forecasting (WRF) model developers to prepare the global 0.5 km land cover type data (**Broxton et al. 2014b**) that was released in the WRF Release in summer 2014.

- Our global 0.5 km land cover type data (**Broxton et al., 2014b**) has also been tested for implementation in CLM5.0 in 2016.

- Our global 1 km bedrock depth data **(Pelletier et al., 2015)** has been tested for implementation in CLM5.0 in 2016.

- Our global 1 km bedrock depth data **(Pelletier et al., 2015)** will be tested for future implementation in the ACME land model Version 2 (ALM2.0).

7. Education and mentoring

- Patrick Broxton received his Ph.D. in December 2013.

- Michael Brunke received his Ph.D. in May 2015.

- Drs. Pieter Hazenberg, Patrick Broxton, and Michael Brunke have been trained and mentored in this interdisciplinary project, and have become promising young scientists in this area.

8. Relevant DOE services

Besides these achievements, we have done the following DOE services:

- PI Zeng served on the review panel of DOE PNNL Climate Change Research Science Focus Area (SFA) proposal, 2012

- Zeng served on the review panel of the DOE Early Career proposals, 2012

- Zeng served on the review panel of the DOE Early Career proposals, 2015

- Zeng served on the review panel of DOE/ORNL terrestrial ecosystem Scientific Focus Area (SFA) proposal, 2015

9. Publications **(that acknowledged the support of our DOE project)**

Broxton, P., P. Troch, M. Schaffner, C. Unkrich, D. Goodrich, 2014a: An All-Season Flash Flood Forecasting System for Real-Time Operations, BAMS, , 95(3), 399-407, DOI: 10.1175/BAMS-D-12-00212.

Broxton, P., X. Zeng, D. Sulla-Menashe, and P. Troch, 2014b: A global land cover climatology using MODIS data. J. Appl. Meteor. Clim, 53, 1593–1605. DOI: 1175/JAMC-D-13-0270.1

Broxton, P., X. Zeng, W. Scheftic, and P. Troch, 2014c: A MODIS-Based Global 1 km Maximum Green Vegetation Fraction Dataset, J. Appl. Meteor. Clim., 53, 1996–2004, DOI: 10.1175/JAMC-D-13-0356.1.

Brunke, M. A., P. Broxton, J. Pelletier, D. Gochis, P. Hazenberg, D. M. Lawrence, L. R. Leung, G.-Y. Niu, P. A. Troch, and X. Zeng, 2015: Implementing and evaluating variable soil thickness in the Community Land Model version 4.5, J. Climate. accepted with revisions.

Hazenberg, P., Y. Fang, P. Broxton, D. Gochis, G.-Y. Niu, J.D. Pelletier, P.A. Troch and X. Zeng, 2015a: A hybrid-3D hillslope hydrological model for use in Earth system models, Water Resour. Res., in press, doi: 10.1002/2014WR016842.

Hazenberg, P., P. Broxton, D. Gochis, G.-Y. Niu, L.A. Pangle, J.D. Pelletier, P.A. Troch and X. Zeng, 2015b: Testing the hybrid-3D hillslope hydrological model in a controlled environment, Water Resour. Res., submitted.

Hazenberg, P., and coauthors, 2015c: Development of hybrid 3-D approach to simulate the hydrological response of the land surface at hyper-resolution, J. Hydrometeor., in preparation.

Niu, G.Y., and X. Zeng, 2012: The Earth System Model, Modeling the land component of. Book Chapter of the Encyclopedia of Sustainability Science and Technology, R.A. Meyers, Ed., doi: 10.1007/978-1-4419-0851-3.

Niu, G.-Y., C. Paniconi, P. A., Troch, R. L. Scott, M. Durcik, X. Zeng, T. Huxman, and D. Goodrich, 2013a: An integrated modeling framework of catchment-scale ecohydrological processes. Part 1: model description and tests over an energy-limited watershed, Ecohydrology, 6, doi: 10.1002/eco.1362.

Niu, G.-Y., P. A. Troch, C. Paniconi, R. L. Scott, M. Durcik, X. Zeng, T. Huxman, D.C. Goodrich, and J. Pelletier, 2013b: An integrated model framework of catchment-scale ecohydrological processes: 2. the role of water subsidy by overland flow on vegetation dynamics in a semi-arid catchment, Ecohydrology, 6, doi: 10.1002/eco.1405.

Niu, G.-Y., D. Pasetto, C. Scudeler, C. Paniconi, M. Putti, P. A. Troch, S. B. DeLong1, K. Dontsova, L. Pangle1, D. D. Breshears, J. Chorover, T. E. Huxman, J. Pelletier, S. R. Saleska, and X. Zeng, 2014: Incipient subsurface heterogeneity and its effect on overland flow generation – insight from a modeling study of the first experiment at the Biosphere 2 Landscape Evolution Observatory, Hydrol. Earth Syst. Sci., 18, 1873–1883, 2014 www.hydrol-earth-syst-sci.net/18/1873/2014/ doi:10.5194/hess-18-1873-2014

Pelletier, J.D., 2013: A robust, two-parameter method for drainage network extraction from high-resolution Digital Elevation Models (DEMs), Water Resour. Res., 49, 1–15, doi:10.1029/2012WR012452.

Pelletier, J.D., P.D. Broxton, P. Hazenberg, X. Zeng, P.A. Troch, G.-Y. Niu, Z.C. Williams, M.S. Brunke, and D. Gochis, 2015: A gridded global dataset of soil, saprolite, and alluvial thicknesses for regional and global land-surface modeling. J. Adv. Modeling Earth Systems, accepted with revisions.

Sakaguchi, K., X. Zeng, and M. Brunke, 2012a: Temporal and Spatial Scale Dependence of IPCC AR4 Climate Models in Simulating the Surface Temperature Trend in the 20th Century. J. Climate, 25, 2456-2470, doi: http://dx.doi.org/10.1175/JCLI-D-11-00106.1.

Sakaguchi, K., X. Zeng, and M. Brunke, 2012b: The Hindcast Skill of the CMIP Ensembles for the Surface Air Temperature Trend. J. Geophys. Res., 117, D16113, doi:10.1029/2012JD017765.

Wang, A., and X. Zeng, 2013: Development of global hourly 0.5-degree land surface air temperature datasets. J. Climate, 26, 7676-7691, doi: 10.1175/JCLI-D-12-00682.1.

Wang, A., and X. Zeng, 2014: Land surface air temperature diurnal range over high northern latitudes. J. Geosphys. Res.-Atmospheres, 119, 5836–5844, doi:10.1002/2014JD021602.

Wang, A. and X. Zeng, 2015: Global Hourly Land Surface Air Temperature Datasets: Inter-comparison and Climate Change. Int. J. Climatol., doi: 10.1002/joc.4257.

Zeng, X., and A. Wang, 2012: What Is Monthly Mean Land Surface Air Temperature? Eos Trans., 93 (15), 156.

Zeng, X., K.L. Kiviat, K. Sakaguchi, and A.M.A. Mahmoud, 2012: A toy model for monthly river flow forecasting. J. Hydrology, 452-453, 226-231, doi: 10.1016/j.jhydrol.2012.05.053.

Zhang, X. G.-Y. Niu, A. S Elshall, M. Ye, G. A. Barron-Gafford, M. Pavao-Zuckerman, 2014: Assessing five evolving microbial enzyme models against field measurements from a semiarid savannah-What are the mechanisms of soil respiration pulses? Geophysical Research Letters (41) 18, 6428-6434, doi: 10.1002/2014GL061399.